Journal of Chromatography B, 895–896 (2012) 146–153

Contents lists available at SciVerse ScienceDirect

Journal of Chromatography B

journal homepage: www.elsevier.com/locate/chromb

Isolation of brefeldin A from *Eupenicillium brefeldianum* broth using macroporous resin adsorption chromatography

Ya-Jun Wang[a,b], Ye-Fei Wu[a,b], Feng Xue[a,b], Zhi-Xian Wu[a,b], Ya-Ping Xue[a,b], Yu-Guo Zheng[a,b,*], Yin-Chu Shen[a,b]

[a] *Institute of Bioengineering, Zhejiang University of Technology, Hangzhou, Zhejiang 310014, PR China*
[b] *Engineering Research Center of Bioconversion and Biopurification, Ministry of Education, Zhejiang University of Technology, Hangzhou 310014, PR China*

ARTICLE INFO

Article history:
Received 16 November 2011
Accepted 25 March 2012
Available online 1 April 2012

Keywords:
Brefeldin A
Macroporous resin
Purification
Adsorption chromatography
Crystallization

ABSTRACT

Brefeldin A (BFA) is a macrolide lactone antibiotic, possessing antitumor, antiviral, antifungal activities. In this work, a separation strategy involving one-step macroporous resin adsorption chromatography combined with crystallization was established for BFA purification from *Eupenicillium brefeldianum* CCTCC M 208113 fermentation broth. Among six macroporous resin adsorbents tested, the non-polar resin HZ830 had the best adsorption and desorption performance. The static equilibrium adsorption data fitted well with the Freundlich equation, and the adsorption kinetic followed the pseudo-second order model. Through experimental optimization of column adsorption and desorption, BFA in purity of 90.4% (w/w), 92.1% (w/w) yield was obtained by a one-step macroporous resin adsorption chromatography, using a stepwise elution protocol. Furthermore, high purity (>99%, w/w) of BFA crystals were prepared from *E. brefeldianum* CCTCC M 208113 fermentation broth in an overall recovery of 67.0% (w/w), using a combination of adsorption chromatography packed with non-polar macroporous adsorbent HZ830 and crystallization in acetone.

1. Introduction

Brefeldin A (BFA) is a 13-carbon macrolide lactone antibiotic firstly isolated from *Penicillium decumbens* by Singleton et al. [1]. It blocks the secretory process in eukaryotic cells by interfering in the endoplasmic reticulum (ER) to Golgi membrane traffic, causing the disassembly of Golgi apparatus and redistribution of Golgi-apparatus proteins into the ER [2,3], contributing to its antifungal and antiviral activities. Besides, BFA can induce a wide variety of human cancer cells to differentiation and apoptosis, such as neuroendocrine tumors [4] and prostatic cancer cells via a p53-independent mechanism [5,6]. It is in the development as a lead anticancer agent [7,8].

Due to its anticancer activity, BFA production via microbial fermentation and chemical synthesis attracted great attentions. The total chemical synthesis of (±)-brefeldin A was firstly reported in 1976 [9]. One decade later, the synthesis of optically pure brefeldin A was completed [10]. Since then, a great number of reports are available on the synthesis of (+)-brefeldin A [11–26]. Despite that significant advances have been made in brefeldin A synthesis, commercial brefeldin A production exclusively relies on microbial fermentation [27–29].

Therefore, developing an efficient BFA separation strategy from fermentation broth is of significant importance. However, there are only limited documents concerning BFA separation and purification. Kim and Kochevar developed a chromatographic method with reversed-phase (C18) silica to isolate BFA from *Penicillium brefeldianis* broth [30]. Recently, high-speed counter-current chromatography (HSCCC), assisted with electrospray ionization mass spectrometry (ESI-MS), was applied to recover BFA from the crude extract of *Penicillium* SHZK-15 culture [31]. Both purification methods suffer low capacity and high cost. So far, no document on the BFA separation using macroporous resin is available. Macroporous resins are widely applied in the separation of antibiotics and other active substances [32–38], attributing to their unique characteristics including relative inexpensiveness, high adsorption capacity, good stability and mild operating conditions.

A BFA overproducing fungus, *Eupenicillium brefeldianum* CCTCC M 208113, was successfully bred from a *M. paniculata* endophytic fungus *E. brefeldianum* A1163 in our previous research [39,40]. The purpose of this research is to investigate the feasibility of purifying BFA from the fermentation broth of *E. brefeldianum* CCTCC M 208113 using a combination of macroporous resin adsorption chromatography and crystallization. The adsorption isotherm,

* Corresponding author at: Institute of Bioengineering, Zhejiang University of Technology, Hangzhou, Zhejiang 310014, PR China. Tel.: +86 571 88320630; fax: +86 571 88320630.
E-mail address: zhengyg@zjut.edu.cn (Y.-G. Zheng).

1570-0232/$ – see front matter © 2012 Elsevier B.V. All rights reserved.
http://dx.doi.org/10.1016/j.jchromb.2012.03.033

adsorption kinetics and breakthrough behavior of BFA on macroporous resin HZ830 were studied in detail.

2. Materials and methods

2.1. Materials

2.1.1. Adsorbents

Six macroporous resins including HZ830, HZ816, HZ818, HZ841, HZ806 and HZ820 were used in this work. All of them were first soaked in 95.0% (v/v) ethanol for 12 h, washed thoroughly with distilled water, and vacuum dried prior to use. Their physical properties and specification are tabulated in Table 1.

2.1.2. Chemicals

Methanol and ethanol were both of analytical reagent grade. Deionized water was purchased from Wahaha Group Co., Ltd. (Hangzhou, China). BFA crystals used in this study were self-made in our laboratory from the fermentation broth of *E. brefeldianum* CCTCC M 208113 [39,40].

2.2. Methods

2.2.1. Resin selection

Resin selection was conducted based on their adsorption and desorption capabilities for BFA. In adsorption experiment, 50.0 mg of each macroporous resin HZ830, HZ816, HZ818, HZ841, HZ806 and HZ820 was weighted into 250 ml flasks and exposed to 100.0 ml of 0.10 mg/ml BFA solution, agitated for 24 h with a blade stirrer at 200 rpm, 30 °C. In the subsequent desorption test, 6 resins saturated with BFA were first washed with deionized water, and then desorbed with 20.0 ml ethanol, by agitating under the same conditions.

The equilibrium adsorption capacity was calculated from the mass balance equation.

$$q_e = \frac{V_1(C_0 - C_e)}{m} \quad (1)$$

where q_e is the equilibrium adsorption capacity (mg/g dry resin), V_1 is the volume of BFA solution (ml), C_0 is the initial concentration of BFA (mg/ml), C_e is the concentration of BFA in solution at equilibrium (mg/ml), and m is the dry weight of resin (g).

The capacities of desorption and the desorption ratio were calculated by

$$q_d = \frac{C_d V_d}{m} \quad (2)$$

$$D(\%) = \frac{q_d}{q_e} \quad (3)$$

where q_d is the desorption capacity (mg/g dry resin), C_d the concentration of BFA in the desorption solution (mg/ml), V_d the volume of the desorption solution (ml) and D the desorption ratio.

2.2.2. Adsorption isotherms

Experiments of adsorption isotherms were conducted at the initial BFA concentrations of 0.02, 0.03, 0.04, 0.05, 0.06, 0.07, 0.08 and 0.10 mg/ml, at temperatures of 293, 303, 313 and 323 K, respectively. 10.0 mg of resin was weighted into each 50 ml flask, to which 50.0 ml BFA solution was added. Adsorption lasted 24 h at 200 rpm.

2.2.3. Adsorption isotherm models

Langmuir and Freundlich models were used to analyze the adsorption isotherms data. The Langmuir isotherm is the most widely used for monolayer adsorption [41]. The Langmuir equation is represented as Eq. (4).

$$q_e = \frac{q_m C_e}{K_L + C_e} \quad (4)$$

where C_e is the concentration of BFA in solution at equilibrium (mg/ml), q_m the theoretical maximum adsorption capacity under experimental condition (mg/g dry resin) and K_L the Langmuir constant.

The Freundlich isotherm [42] is an empirical equation employed to describe multilayer adsorption with interaction between adsorbed molecules, represented as Eq. (5).

$$q_e = K_F C_e^{1/n} \quad (5)$$

where K_F and n are the Freundlich constants. Depending on the values of n, the adsorption behavior can be classified as favorable ($n > 1$), irreversible ($n = 1$) and unfavorable ($n < 1$) [43].

2.2.4. Adsorption kinetics

For the kinetic studies, 500.0 ml BFA solution (0.10 mg/ml) was introduced into a 500 ml conical flask containing 0.50 g of the dried absorbent HZ830, with liquid level of 9.2 cm. The suspension was agitated at 400 rpm for 10 h with a blade stirrer at temperatures of 293, 303 and 313 K. During the adsorption, an aliquot of 0.50 ml was withdrawn for BFA detection, at an interval of 10 min till equilibrium.

2.2.5. Adsorption kinetic models

Four kinetic model equations including the pseudo-first order, pseudo-second order, liquid film diffusion and intra-particle diffusion models were used to analyze the adsorption data.

2.2.5.1. Pseudo-first order rate equation. The pseudo-first-order kinetic model, established by Lagergren, is the most widely used rate equation in liquid phase adsorption [44], written as Eq. (6).

$$\log(q_e - q_t) = \log\ q_e - \left(\frac{K_1}{2.303}\right) t \quad (6)$$

where K_1 is a constant for the pseudo-first order rate equation, q_e the equilibrium adsorption capacity, q_t the adsorption capacity at time t.

2.2.5.2. Pseudo-second order rate equation. The second-order rate equation [45,46] can be expressed as Eq. (7).

$$\frac{t}{q_t} = \frac{1}{K_2 q_e^2} + \frac{t}{q_e} \quad (7)$$

where K_2 is a constant for the pseudo-second order rate equation.

2.2.5.3. Liquid film diffusion model. The kinetic model of external liquid film diffusion can be expressed as Eq. (8) [47,48].

$$-\ln\left(1 - \frac{q_t}{q_e}\right) = K_3 t \quad (8)$$

where K_3 is a constant for the liquid film diffusion model.

2.2.5.4. Intra-particle diffusion model. The intra-particle diffusion model was developed by Weber [49,50], expressed as Eq. (9).

$$q_t = K_4 t^{0.5} + C \quad (9)$$

where K_4 is a constant for the intra-particle diffusion model. The plot of q_t versus $t^{0.5}$ may present multi-linearity, which demonstrates that more than one rate-controlling steps exist in the adsorption process [51].

Table 1
Physical properties of the test macroporous resins.

Trade name	Average pore diameter (Å)	Surface area ($m^2\ g^{-1}$)	Particle size (mm)	Polarity
HZ 816	60–70	730–800	0.3–1.2	Non-polar
HZ 818	70–80	880–920	0.3–1.0	Non-polar
HZ 820	80–90	680–800	0.3–1.2	Non-polar
HZ 830	85–95	780–820	0.4–1.0	Non-polar
HZ 841	85–95	500–600	0.4–1.2	Weak-polar
HZ 806	60–70	480–620	0.3–1.2	Medium-polar

2.2.6. Effect of initial BFA concentration and agitation rate on adsorption process

To study the impact of initial BFA concentration on adsorption process, 500.0 ml of BFA solution at concentrations of 2.5×10^{-2}, 3.7×10^{-2}, 5.0×10^{-2} mg/ml was transferred into each 500 ml conical flask containing 0.50 g of the pretreated sorbent HZ830 with liquid level of 9.2 cm. The suspension was agitated for 10 h with a blade stirrer at 400 rpm, 303 K. An aliquot of 0.50 ml was withdrawn for the detection of BFA in the liquid phase. In a similar way, influence of agitation rate on adsorption process was conducted at 100, 200, 300 and 400 rpm at an initial BFA concentration of 0.050 mg/ml.

2.3. Dynamic adsorption and desorption

The glass columns (1.5 cm ID, 18 cm length) were used in the dynamic adsorption and desorption experiments, which were wet-packed with wet adsorbent HZ830 (4.5 g, dry weight) at a BV (bed volume) of 20.0 ml. The dynamic breakthrough experiments were carried out at 303 K. Effect of feed BFA concentration was examined in a range of 0.05, 0.07 and 0.10 mg/ml, at a flow rate of 0.08 BV/min. Samples were collected for BFA detection in effluent. Effect of flow rate on breakthrough curves was examined in a similar way, ranging between 0.03 and 0.08 BV/min, at feed concentration of 0.050 mg/ml.

For dynamic desorption, the column saturated with BFA was first washed with 2.0 BV of deionized water, then eluted by various ethanol–water solutions at volumetric ratios of 30:70 (v/v), 40:60 (v/v) and 50:50 (v/v), at varying elution rates of 0.02 BV/min, 0.03 BV/min, 0.04 BV/min and 0.05 BV/min, respectively. Eluates were collected for BFA detection.

2.4. Stepwise elution

The BFA fermentation broth of *E. brefeldianum* CCTCC M 208113 was made in our laboratory [39,40]. Fermentation broth was centrifuged at 9000 rpm for 10 min to remove the mycelia and other insoluble impurities. Thereafter, 2.0 l of clarified supernatant was pumped at a flow rate of 0.03 BV/min, into the chromatography column pre-packed with adsorbent HZ830 at a BV of 20.0 ml. Elution was conducted using a stepwise elution protocol. After sample loading, 2 BV of deionized water was used to wash the column in the first step, followed by elution with 4 BV of 50% (v/v) ethanol aqueous solution, and finally the column was regenerated with ethanol. Eluates were collected for BFA detection.

2.5. Crystallization

Eluate containing BFA, collected during the second stage of stepwise elution, was combined. After removal of solvent under vacuum dried, the crude product was dissolved in 10 volumes of acetone, filtrated through filter paper. On evaporation of the acetone at room temperature, crystals emerged from the clarified solution. The first crystals were collected, redissolved in acetone, and recrystallized [40].

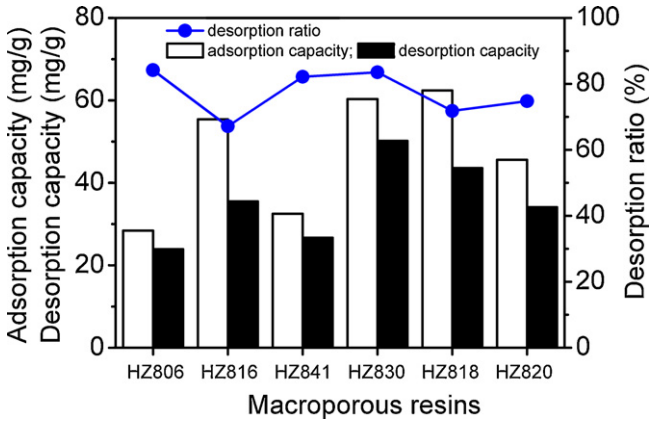

Fig. 1. Adsorption and desorption capacities of BFA on macroporous resins.

2.6. Analytical methods

Brefeldin A content was analyzed using a Shimadzu LC-10AT HPLC system, which consists of a manual 20 μl loop injector, a LC-20AD pump and SPD-20A detector. Separation was achieved on a Rascil C18 column (4.6 mm × 25 cm). The mobile phase was composed of methanol aqueous solution at a volumetric ratio of 70:30, and run at a flow rate of 0.60 ml/min. Absorbance detection wavelength was set at 230 nm. Each sample was microfiltered through 0.45 μm membrane, and, a 20.0 μl of the resulting filtrate was loaded into the HPLC system for a single run.

Each run of culture experiments and analysis was replicated thrice to ensure consistency and accuracy. Hence, data obtained for a specific experimental condition are the results of three separate batch experiments, and provided as mean ± standard deviation.

3. Results and discussion

3.1. Adsorption and desorption examination

Adsorption and desorption capacities of the macroporous resins HZ806, HZ816, HZ818, HZ820, HZ830 and HZ841 for BFA were measured, as shown in Fig. 1. Among the six adsorbents tested, non-polar macroporous resins HZ830, HZ818 had higher adsorption capacity for BFA, reaching 60.3 and 62.4 mg/g dry resin, respectively, accounting for a high degree of compatibility between adsorbent and BFA. Besides, as shown in Table 1, the adsorbent HZ818 has the highest surface area, accounting for its highest adsorption capacity among all of the non-polar resins tested. BFA desorption experiments demonstrated that ethanol is efficient to desorb BFA. The large average pore diameter can make desorption progress take place much easily [52], contributing to resin HZ830 had the highest desorption ratio of 83.9%; in contrast, within 24 h, the desorption ratio of BFA from HZ818 resin was as low as 68.8%, related with its relative small average pore diameter. As the amount by the wash loss after adsorption is negligible, the BFA leftover is presumably bound to the resin at desorption equilibrium. However, the leftover amount in each run was found to

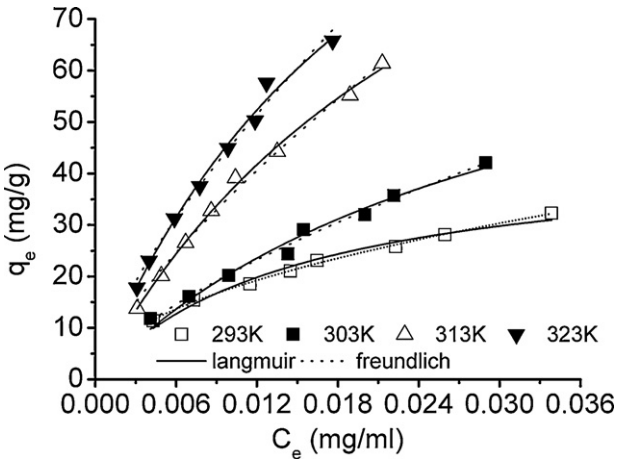

Fig. 2. Adsorption isotherms of BFA on macroporous resin HZ830. Adsorption experiments were conducted at initial BFA concentrations between 0.02 mg/ml and 0.1 mg/ml, agitation speed of 200 rpm.

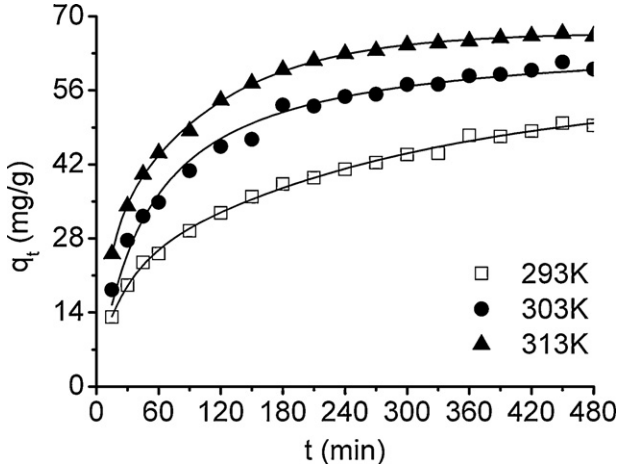

Fig. 3. Dynamic curves of BFA adsorption on macroporous resin HZ830. Adsorption experiments were conducted at initial BFA concentration of 0.10 mg/ml, agitation speed of 400 rpm.

be close and no significant changes were observed in repeated batch adsorption–desorption experiments. Kim and Kochevar used methanol to elute BFA from C18 silica [30]. Obviously, ethanol is a better option over methanol for the consideration of better safety. Due to its high adsorption and desorption capacity, non-polar macroporous resin HZ830 was used for BFA isolation in subsequent investigation.

3.2. Adsorption isotherms

The adsorption isotherm was studied in a temperature range of 293–323 K. Obviously, the BFA adsorption increased with increasing temperature, as shown in Fig. 2. Langmuir model and Freundlich model were used to fit the experimental data of BFA equilibrium adsorption on non-polar macroporous adsorbent HZ830. As shown in Table 2, fitting with Freundlich equation yielded a higher correlation coefficient (R^2) than that of Langmuir model, demonstrating that the Freundlich model better describes this BFA adsorption equilibrium. Moreover, evident deviations between the theoretical q_e fittings with Langmuir equation and the experimental values were seen. For Freundlich model, n values are higher than 1, indicating that absorbent has a higher affinity for BFA than the liquid phase and BFA can be easily captured by the resin. Since the K_F values increased with temperature, raising temperature is preferred with regards to equilibrium adsorption capacity.

3.3. Adsorption kinetic study

Kinetic studies were performed in a temperature range of 303–323 K, as shown in Fig. 3. BFA was rapidly captured in the initial 60 min, thereafter a slowdown in adsorption rate was observed. BFA adsorption reached the equilibrium at 6 h. In order to provide sufficient information about BFA adsorption, four kinetic models including pseudo-first order, pseudo-second order, liquid film diffusion and intra-particle diffusion models were used to analyze the kinetic data.

3.3.1. Pseudo-first-order and pseudo-second-order

Compared with the pseudo-first order model, the pseudo-second order model yielded better linear correlation, shown in Fig. 4(a) and (b), and the theoretical q_e values were coincident with the experimental $q_{e,exp}$ values (Table 3). Besides, the pseudo-second-order is superior as R^2 values approaching to unity.

3.3.2. Liquid film diffusion model

Fig. 4(c) presents the relationship between $-\ln(1-q_t/q_e)$ and t. Obviously, $-\ln(1-q_t/q_e)$ had a good linear correlation with t, but the straight line did not pass through the origin, suggesting that adsorption rate is controlled by the liquid film thickness at the beginning of this adsorption process.

3.3.3. Intra-particle diffusion model

As shown in Fig. 4(d), the plot of q_t versus $t^{1/2}$ presented multi-linearity. The presence of three linear sections versus the square root of time, $t^{1/2}$, means there were three rate-controlling steps during BFA adsorption. An explanation for this phenomenon is that the intra-particle diffusion is controlled by three categories of adsorbent pores, namely macropores, mesopores and micropores [53]. The first linear region is most likely due to the adsorption occurred in the macropores. Adsorption can take place easily in this region due to the small diffusion resistance. The second rate-controlling step was mesopore diffusion. The slope of the second linear section became smaller, demonstrating that the diffusion resistance in mesopores increased. For BFA, about 4 h was required for reaching the adsorption equilibrium in the micropores of adsorbent HZ830, accounting for the slope is much smaller than that of the second linear section. Hence, we concluded that the diffusion rate is determined by the pore sizes.

3.4. Effect of initial concentration on adsorption rate

Effect of initial BFA concentration on adsorption rate is illustrated in Fig. 5. Feed concentration notably affected BFA adsorption kinetics. When the initial concentration of BFA increased from 0.025 to 0.05 g/ml, the values of t/q_t became smaller within the same contact time, which indicates that non-polar macroporous adsorbent HZ830 had higher adsorption efficiency at elevated initial concentrations. Our interpretation of this result is that rising feed BFA concentration increases driving force of BFA transport, causing enhanced BFA diffusion through the liquid film surrounding the adsorbent particles.

3.5. Effect of agitation rate on adsorption rate

As shown in Fig. 6, mixing significantly affected adsorption kinetics. The t/q_t values decreased as the agitation rate increased from 100 to 300 rpm, indicating higher agitation speeds are advantageous to BFA adsorption kinetics. The reason is that the

Table 2
Parameter fittings with Langmuir and Freundlich models at varying temperatures.

Isotherm model	*Temp.* (K)	Regression equation	Model parameters		
			K_L	q_m (mg/g)	R^2
Langmuir	293	$\frac{C_e}{Q_e} = 0.85 + 0.0223C_e$	26.13	44.78	0.9756
	303	$\frac{C_e}{Q_e} = 0.37 + 0.0115C_e$	31.08	86.76	0.9788
	313	$\frac{C_e}{Q_e} = 0.20 + 0.0070C_e$	34.12	143.61	0.9905
	323	$\frac{C_e}{Q_e} = 0.15 + 0.0064C_e$	42.33	155.4	0.9907
Isotherm model	*Temp.* (K)	Regression equation	Model parameters		
			K_F	n	R^2
Freundlich	293	$Q_e = 4.72C_e^{0.4975}$	4.72	2.01	0.9974
	303	$Q_e = 6.19C_e^{0.6578}$	6.19	1.52	0.9909
	313	$Q_e = 7.94C_e^{0.7199}$	7.94	1.39	0.9931
	323	$Q_e = 10.33C_e^{0.8475}$	10.33	1.18	0.9892

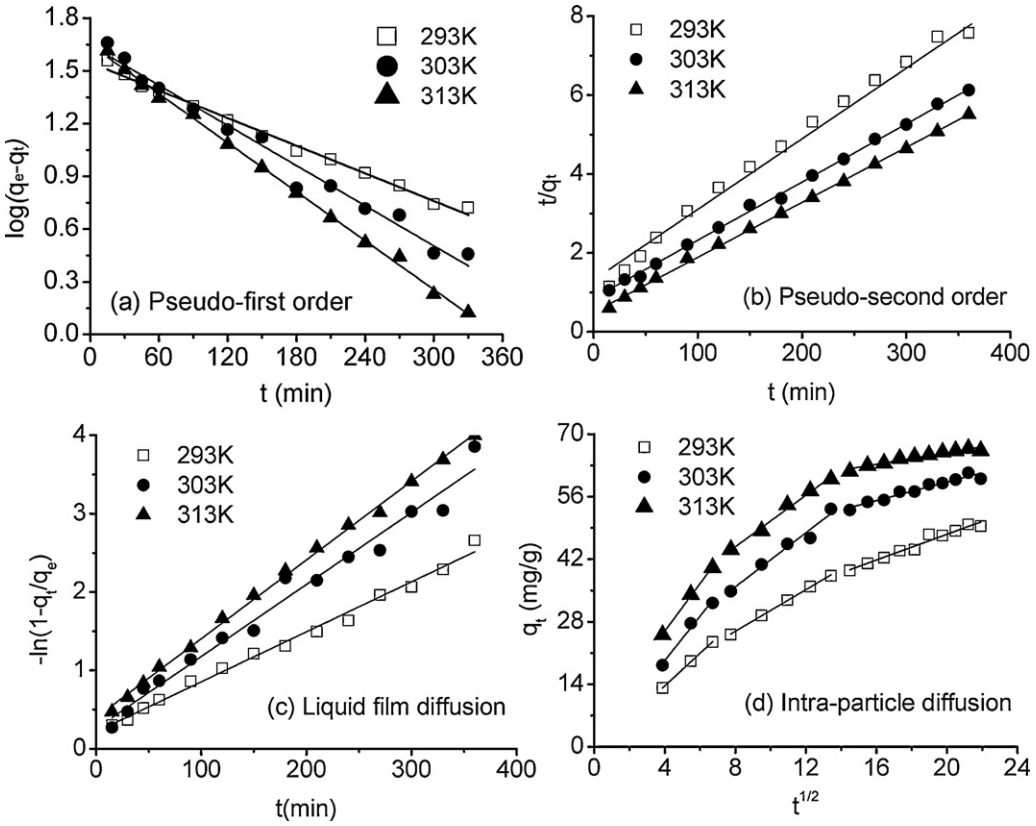

Fig. 4. Fittings of BFA adsorption kinetic parameters at varying temperatures.

Table 3
Temperature dependence of adsorption kinetic parameter fittings.

Kinetic model	*Tem.*	Kinetic parameters		
		K_1	q_e (mg/g)	R^2
Pseudo-first-order: $log(q_e - q_t) = \log q_e - \left(\frac{K_1}{2.303}\right) t$	293 K	6.03×10^{-3}	35.23	0.989
	303 K	8.77×10^{-3}	44.34	0.979
	313 K	1.07×10^{-2}	44.51	0.992
Kinetic model	*Tem.*	Kinetic parameters		
		K_2	q_e (mg/g)	R^2
Pseudo-second-order: $\frac{t}{q_t} = \frac{1}{K_2 q_e^2} + \frac{t}{q_e}$	293 K	2.60×10^{-4}	51.91	0.993
	303 K	2.97×10^{-4}	62.91	0.999
	313 K	4.37×10^{-4}	69.75	0.999

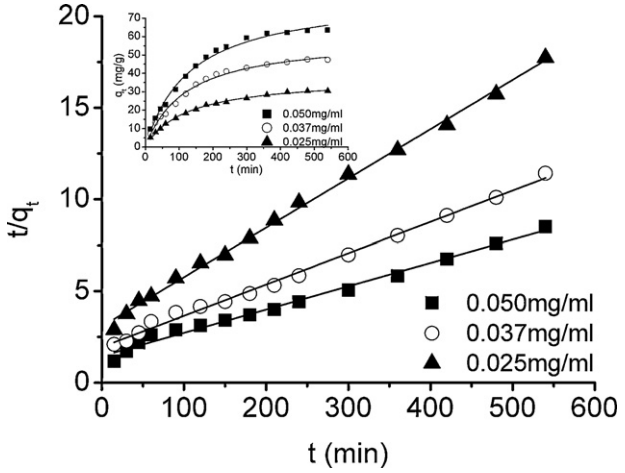

Fig. 5. Effect of initial BFA concentration on adsorption rate. Adsorption experiments were conducted at agitation rate of 400 rpm, 30 °C.

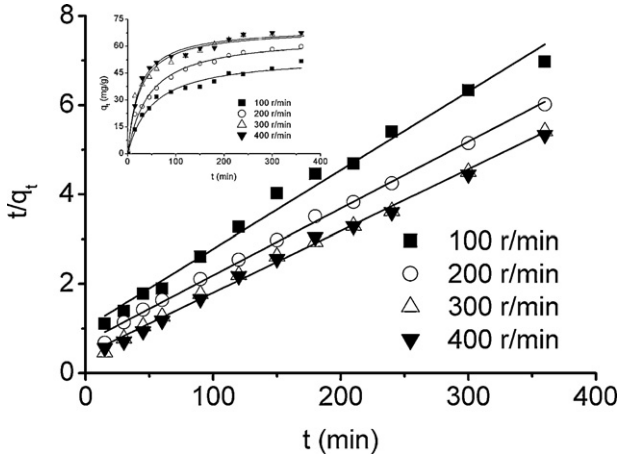

Fig. 6. Effect of agitation rate on BFA adsorption rate. Adsorption experiments were conducted at initial BFA concentration of 0.050 mg/ml, 30 °C.

liquid film surrounding the resin particles becomes thinner under stronger agitation. Moreover, no significant increase in adsorption rate was observed when the agitation rate increased from 300 to 400 rpm, suggesting that external film mass transfer resistance is negligible at sufficient mixing. Hence, agitation at no less than 300 rpm is required to minimize the external diffusion resistance.

3.6. Dynamic breakthrough curve on macroporous resin HZ830

The breakthrough curves at varying feed BFA concentrations in a range of 0.05–0.10 mg/ml were examined, as shown in Fig. 7(a). At the initial concentration of 0.10 mg/ml, better breakthrough was observed with a dynamic adsorption capacity of 48.7 mg/g dry resin, linked with enhanced driving force of mass transfer at higher feed concentration. Effect of flow rate on breakthrough is illustrated in Fig. 7(b). Reducing flow rate from 0.08 to 0.03 BV/min yielded better adsorption performance. Our interpretation of this outcome is that sufficient contact time is required for adsorbate diffusion into resin pores, and incomplete adsorption would occur at too high flow rates. Similar results were observed in the separation of madecassoside and asiaticoside from *Centella asiatica* extracts with resin HPD100 [52].

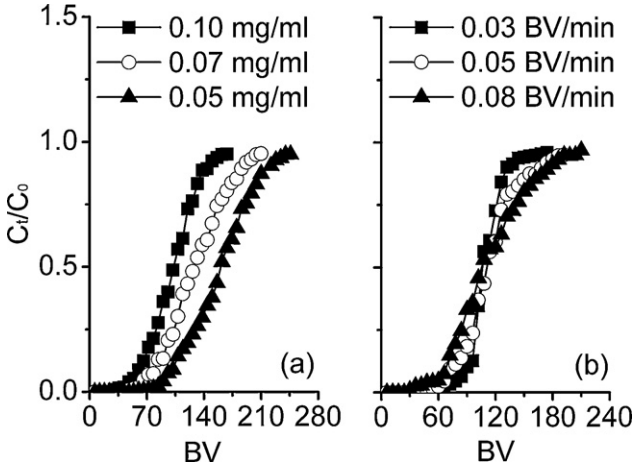

Fig. 7. Effect of initial BFA concentration and flow rate on breakthrough. Operating conditions: bed volume of 20.0 ml, 30 °C; (a) flow rate at 0.08 BV/min; and (b) feed BFA concentration at 0.05 mg/ml.

3.7. Dynamic desorption curve on resin HZ830

Impact of inlet BFA concentration and flow rates on dynamic desorption was investigated at chromatography column packed with non-polar macroporous adsorbent HZ830. As shown in Fig. 8(a), nearly all of the BFA were desorbed in 5 BV when eluted by 50% (v/v) ethanol aqueous solution; reducing ethanol concentration in the eluant brought about longer elution times and serious peak broadening.

Effect of flow rates on dynamic desorption is shown in Fig. 8(b). The elution peak was precipitous and symmetry at low flow rate of 0.02 BV/min, and BFA was completely desorbed in 5 BV. Raising flow rate increased eluant consumption. The phenomena of decreasing flow rate resulted in the increase of the external mass transfer resistance [54] was not obvious in this study, relating to the strong affinity of 50% (v/v) ethanol aqueous solution for BFA and insignificant external mass transfer resistance at low BFA concentrations. In conclusion, the preferential desorption condition for BFA were 50% (v/v) ethanol aqueous solution as eluant, flow rate of 0.02 BV/min.

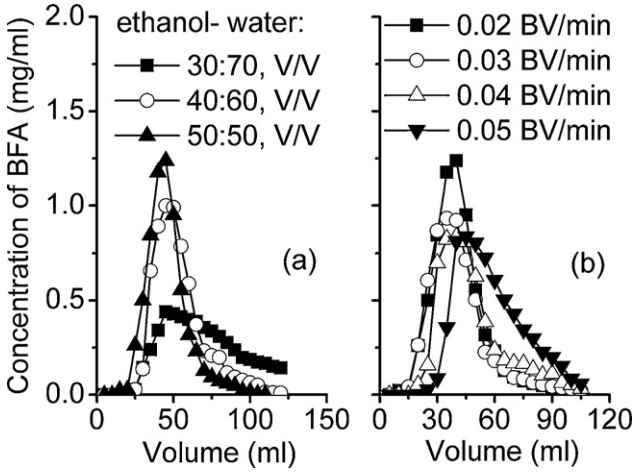

Fig. 8. Effect of inlet BFA concentration and flow rate on elution curves. Operating conditions: bed volume of 20.0 ml, 30 °C; (a) flow rate at 0.02 BV/min; and (b) 50% (v/v) ethanol aqueous solution.

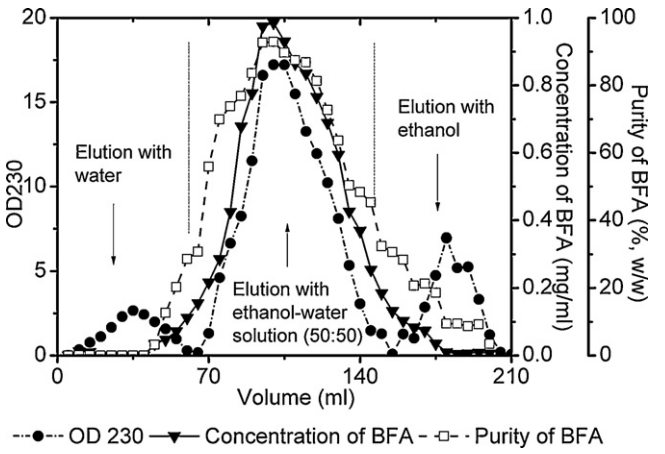

Fig. 9. BFA elution efficiency from column packed with macroporous resin HZ830 using a stepwise elution protocol. Operating conditions: bed volume of 20.0 ml, flow rate of 0.02 BV/min, 30 °C.

3.8. Stepwise elution test

Stepwise elution can make desorption more efficient [52]. In this work, a three-stepwise elution protocol was applied, as shown in Fig. 9. In the first stage, the unbound impurities were quickly eluted by distilled water while BFA was still bound to resin. In the second stage, after eluant was changed to 50% (v/v) ethanol aqueous solution, nearly all of the bound BFA was desorbed within 5 BV. In the third stage, adsorbent HZ830 was regenerated by ethanol. The huge polarity difference between BFA and other substances in the *E. brefeldianum* CCTCC M 208113 broth makes BFA well separated from other impurities. This one-step column chromatography recovered 92.1% (w/w) of BFA with a purity of 90.4% (w/w), demonstrating that it is highly efficient to enrich and purify brefeldin A directly from fermentation broth. The resultant BFA samples were subjected to crystallization and recrystallization in acetone, yielding colorless prism crystals. Recrystallization reduced the overall recovery from broth to 67.0% (w/w). Analyzed by HPLC, the purity of the final BFA product was over 99% (w/w).

4. Conclusion

In this study, macroporous resin is firstly successfully applied to isolate BFA from the fermentation broths of *E. brefeldianum* CCTCC M 208113. Non-polar macroporous adsorbent HZ830 has highest adsorption and desorption capacities among the six test resins. The static adsorption equilibrium follows Freundlich isotherm model. BFA is efficiently recovered and enriched from *E. brefeldianum* CCTCC M 208113 broth by using column chromatography packed with adsorbent HZ830. Further combined with crystallization and recrystallization in acetone, high purity (>99%, w/w) of BFA crystals are prepared. In summary, a separation strategy involving one-step macroporous resin adsorption chromatography and crystallization was successfully established for BFA purification from *E. brefeldianum* CCTCC M 208113 fermentation broth.

Nomenclature

q_e	amount of BFA adsorbed at equilibrium (mg/g dry resin)
q_d	desorption capacity (mg/g dry resin)
V_1	volume of BFA solution (ml)
V_d	volume of the desorption solution (ml)
m	dry weight of resin (g)
C_0	initial concentration of BFA (mg/ml)
C_e	concentration of BFA in solution at equilibrium (mg/ml)
C_d	concentration of BFA in the desorption solution (mg/ml)
D	desorption ratio (%)
q_m	theoretical maximum BFA adsorption capacity under experimental condition (mg/g dry resin)
K_L	Langmuir isotherm constant
K_F; n	Freundlich isotherm constants
T	temperature (K)
q_t	amount of BFA adsorbed at time t
K_1	constant for the pseudo-first order rate equation
K_2	constant for the pseudo-second order rate equation
K_3	constant for the liquid film diffusion model
K_4; C	constants for the intra-particle diffusion model

Acknowledgements

This work was financially supported by 973 Program (No. 2011CB710800), the Major Program for Key Science and Technology of Zhejiang Province of China (2009C13G2020012), and Natural Science Foundation of Zhejiang Province of China (No. Y4090605).

References

[1] V.L. Singleton, N. Bohonos, A.J. Ullstrup, Nature 181 (1958) 1072.
[2] Z. Kossaczka, J. Drgonova, B. Podobova, V. Betina, V. Farkas, Can. J. Microbiol. 41 (1995) 971.
[3] B. Satiatjeunemaitre, C. Hawes, Biol. Cell 74 (1992) 325.
[4] D.E. Larsson, H. Lovborg, L. Rickardson, R. Larsson, K. Oberg, D. Granberg, Anticancer Res. 26 (2006) 4125.
[5] J.R. Chapman, H. Tazaki, C. Mallouh, S. Konno, Mol. Urol. 3 (1999) 11.
[6] E. Wallen, R.G. Sellers, D.M. Peehl, J. Urol. 164 (2000) 836.
[7] R.G. Shao, T. Shimizu, Y. Pommier, Exp. Cell Res. 227 (1996) 190.
[8] J.W. Zhu, H. Nagasawa, F. Nagura, S.B. Mohamad, Y. Uto, K. Ohkura, H. Hori, Bioorg. Med. Chem. 8 (2000) 455.
[9] E.J. Corey, R.H. Wollenberg, Tetrahedron Lett. 17 (1976) 4705.
[10] B.M. Trost, J. Lynch, P. Renaut, D.H. Steinman, J. Am. Chem. Soc. 108 (1986) 284.
[11] S. Archambaud, K. Aphecetche-Julienne, A. Guingant, Synlett (2005) 139.
[12] S. Archambaud, F. Legrand, K. Aphecetche-Julienne, S. Collet, A. Guingant, M. Evain, Eur. J. Org. Chem. (2010) 1364.
[13] E.J. Corey, P. Carpino, Tetrahedron Lett. 31 (1990) 7555.
[14] S. Forster, E. Persch, O. Tverskoy, F. Rominger, G. Helmchen, C. Klein, B. Gonen, B. Brugger, Eur. J. Org. Chem. (2011) 878.
[15] M. Inai, T. Nishii, S. Mukoujima, T. Esumi, H. Kaku, K. Tominaga, H. Abe, M. Horikawa, T. Tsunoda, Synlett (2011) 1459.
[16] D.J. Kim, J.K. Lee, P.J. Shim, J.I. Lim, H. Jo, S.H. Kim, J. Org. Chem. 67 (2002) 764.
[17] M.Y. Kim, H. Kim, J. Tae, Synlett (2009) 1303.
[18] W.M. Lin, C.K. Zercher, J. Org. Chem. 72 (2007) 4390.
[19] S.Y. Seo, J.K. Jung, S.M. Paek, Y.S. Lee, S.H. Kim, Y.G. Suh, Tetrahedron Lett. 47 (2006) 6527.
[20] G. Solladie, O. Lohse, J. Org. Chem. 58 (1993) 4555.
[21] Y.G. Suh, J.K. Jung, S.Y. Seo, K.H. Min, D.Y. Shin, Y.S. Lee, S.H. Kim, H.J. Park, J. Org. Chem. 67 (2002) 4127.
[22] B.M. Trost, M.L. Crawley, J. Am. Chem. Soc. 124 (2002) 9328.
[23] Y.C. Wang, D. Romo, Org. Lett. 4 (2002) 3231.
[24] Y. Wu, J. Gao, Org. Lett. 10 (2008) 1533.
[25] Y.K. Wu, X. Shen, Y.Q. Yang, Q. Hu, J.H. Huang, J. Org. Chem. 69 (2004) 3857.
[26] Y.K. Wu, X. Shen, Y.Q. Yang, Q. Hu, J.H. Huang, Tetrahedron Lett. 45 (2004) 199.
[27] C.C. Howard, R.A.W. Johnstone, I.D. Entwistle, US Patent 3,896,002, (1975).
[28] T.G. Mccloud, M.P. Burns, F.D. Majadly, G.M. Muschik, D.A. Miller, K.K. Poole, J.M. Roach, J.T. Ross, W.B. Lebherz, J. Ind. Microbiol. 15 (1995) 5.
[29] W.Y. Liu, M.J. Fang, P.X. Xu, Y.J. Huang, Y.F. Zhao, Microbiologica 32 (2005) 52 (in Chinese).
[30] H.L. Kim, J. Kochevar, Gen. Pharmacol. 26 (1995) 363.
[31] P.X. Xu, X. Gao, R.Q. Zhuang, J.N. Guo, J. Bao, M.J. Fang, Y. Liu, Y.F. Zhao, J. Sep. Sci. 33 (2010) 277.
[32] Y.F. Liu, D.L. Di, Q.Q. Bai, J.T. Li, Z.B. Chen, S. Lou, H.L. Ye, J. Agric. Food Chem. 59 (2011) 9629.
[33] B. Zhang, R.Y. Yang, Y. Zhao, C.Z. Liu, J. Chromatogr. B 867 (2008) 253.
[34] H. Ni, X.H. Zhou, H.H. Li, W.F. Huang, J. Chromatogr. B 877 (2009) 2135.
[35] B.Q. Fu, J. Liu, H. Li, L. Li, F.S.C. Lee, X.R. Wang, J. Chromatogr. A 1089 (2005) 18.
[36] A.R. Patil, V.G. Gaikar, Ind. Eng. Chem. Res. 50 (2011) 7452.
[37] F.J. Yang, M. Yang, Y.J. Fu, Y.G. Zu, M. Luo, W. Wang, C.B. Gu, J. Med. Plants Res. 5 (2011) 1741.
[38] Z.Q. Meng, G. Ding, Y.J. Liu, J. Xu, W.J. Liu, W. Xiao, China J. Chin. Mater. Med. 36 (2011) 1007.
[39] Y.G. Zheng, Y.J. Wang, F. Xue, Y.P. Xue, Y.C. Shen, *Eupenicillium brefeldianum* ZJB082702 and application thereof in brefeldin A fermentation, China Patent ZL 2008 1 0163775.5. (December 31, 2008).

[40] Y.G. Zheng, F. Xue, Y.J. Wang, Y.P. Xue, Y.C. Shen, Chin. J. Antibiot. 34 (2009) 593.
[41] I. Langmuir, JACS 38 (1916) 2221.
[42] H. Freundlich, J. Phys. Chem. 57 (1907) 385.
[43] S.D. Faust, O.M. Aly, Butterworth (1987).
[44] S. Lagergren, Kungliga Svenska Vetenskapsakademiens. Handlingar 24 (1898) 1.
[45] Y.S. Ho, G. Mckay, Adsorpt. Sci. Technol. 16 (1998) 243.
[46] Y.S. Ho, G. McKay, Process Biochem. 34 (1999) 451.
[47] G.E. Boyd, A.W. Adamson, L.S. Mayers, JACS 69 (1947) 2836.
[48] A. Torrado, M. Valiente, Solvent Extr. Ion Exch. 26 (2008) 240.
[49] W.J. Weber, J.C. Morris, J. Sanit. Eng. Div. 89 (1963) 31.
[50] K.K.H. Choy, J.F. Porter, G. McKay, J. Chem. Eng. Jpn. 103 (2004) 133.
[51] B.A. Bell, A.H. Molof, Water Res. 9 (1975) 857.
[52] G. Jia, X. Lu, J. Chromatogr. A 1193 (2008) 136.
[53] E. Tutem, R. Apak, C.F. Unal, Water Res. 32 (1998) 2315.
[54] Y. Liu, J. Liu, X. Chen, Y. Liu, D. Di, Food Chem. 123 (2010) 1027.